# Collision-free Motion Coordination of Unicycle Multi-agent Systems

D. Kostić, S. Adinandra, J. Caarls, and H. Nijmeijer, *Fellow*, *IEEE*

***Abstract*—We propose a method for collision-free motion coordination of a group of unicycle agents. Under constraints on control signals, this method guarantees asymptotic tracking of the reference trajectories of all individual agents. The motion coordination is established by mutual coupling of coordinates of the interacting agents. For stronger couplings, the robustness of motion coordination to perturbations is increased. A collision avoidance algorithm is formulated to gain additional robustness against perturbations. The proposed control method is successfully validated in experiments.**

***Index Terms*—Coordinated control, control of non-holonomic systems, stability of nonlinear systems, collision avoidance.**

## I. Introduction

MOTION coordination is a way to control a group of autonomous robots or vehicles (hereafter multi-agent systems). In this paper we address the motion coordination by deriving and implementing a novel control algorithm which solves the problem where multi-agent non-holonomic systems are required to follow predefined trajectories while maintaining a desired spatial pattern. In this algorithm, the motion of each agent is governed based on its own state and the state of its "neighbors". A mechanism for collision avoidance is introduced, such as to enhance applicability of the control algorithm in practice.

In many applications coordinated multi-agent systems of simple structure can be employed to accomplish complex tasks. These systems may increase efficiency, robustness, cost-savings and safety of task execution in comparison with performance of a more complex single system or human. Motion coordination of multi-agent systems, like formation keeping, can be applied in spatially distributed tasks, such as transportation in warehouses, security patrols, search and rescue, etc. Group coordination and multi-agent cooperative control are actively researched in the recent years [1-3].

For example, autonomous agents (mobile robots or unmanned aerial vehicles) can increase robustness of transportation of goods in warehouses with respect to use of conveyers, since trajectories of the mobile units can dynamically be altered such as to avoid obstacles and successfully accomplish given transportation tasks. The planning and scheduling of the tasks can be done centrally, but in a more flexible approach the agents could negotiate with each other and with the supervisor such as to achieve robustness to different types of failures. A high-level multi-agent coordination can be solved using a holonic approach [4,5]. Holons [6] are autonomous controllers that cooperate in order to achieve a common goal. By motion coordination of the agents, the throughput of the transportation can be optimized. The coordination may involve spatial patterning of the agents, such as formation of platoons. Other examples of patterning can be encountered during cooperative manipulation of a massive object by a formation of the coordinated agents; the agents manipulate the object while establishing grasping, caging, or conditional closure patterns [7].

Different approaches to formation control of multi-agent systems can be found in the literature [1-3]: leader-follower, behavior-based strategy, a potential-field approach, a virtual structure approach, use of generalized coordinates, model-predictive control, neural-network and fuzzy-logic strategies, etc. In some approaches particular attention is given to the stabilization and tracking control of mobile agents that belong to the class of nonholonomic dynamical systems. Such systems do not satisfy Brockett's necessary condition for smooth stabilization [8], so no smooth time-invariant stabilizing control law exists for these systems. A great deal of the research aims at developing suitable time-varying stabilizing and tracking controllers for single nonholonomic systems, see for instance [9-11] and the references therein. With just a few exceptions, e.g. [10,11] and some references therein, the stabilization and tracking problems with saturation constraints on control signals have rarely been addressed in the literature, although such constraints are often encountered in practice degrading both stability and performance of tracking control.

In this paper we propose a control strategy for motion coordination of agents featuring nonholonomic kinematics of a unicycle [9-11]. Examples of such agents are wheeled mobile robots, unmanned aerial vehicles and tactical missiles. We address the problem where the reference trajectories of interacting agents form a spatial pattern whose shape can change in time (a time-varying formation). The control strategy, proposed in this paper, achieves globally asymptotically stable tracking of these trajectories and coordination between the interacting agents, both under constraints on the actuator inputs. The coordination takes care that after perturbation of one or several agents, the formation is recovered even before the tracking errors of all individual agents converge to zero. The proposed strategy is an extension of the control design presented in [11], in terms of mutual coupling of motion controllers of the individual agents. The controller couplings yield robustness of the formation to perturbations. The design given in [11] does not offer robust formation recovery. Robustness is further strengthened by means of an algorithm for collision avoidance. This algorithm runs at each agent locally and is based on the concept of the artifi-

Manuscript received September 15, 2009.

All authors are with the Section Dynamics and Control, Department of Mechanical Engineering, Technische Universiteit Eindhoven, 5600 MB, Eindhoven, The Netherlands (phone: 31402478332; fax: 31402461418; e-mail: {d.kostic, s.adinandra, j.caarls, h.nijmeijer}@tue.nl).

Preprint submitted to 2010 American Control Conference.
Received September 28, 2009.

cial potential functions [12]. The collision avoidance is achieved by real-time modifications of the reference trajectories of the individual agents. The modification method is more general than the one proposed in [11].

The main contributions of the paper are: *i*) Lyapunov based design of saturated feedback tracking controllers that achieve global asymptotic stable motion coordination of multi-agent unicycle systems, *ii*) global asymptotic tracking of time-varying formations, where the forward and steering velocities of the individual agents can all be mutually different, while the steering velocities can even be discontinuous, *iii*) flexible controller tuning and intuitive adjustment of robustness of motion coordination with respect to perturbations, *iv*) real-time collision avoidance, and *v*) experimental verification.

In section 2 we present background mathematical models and tools. In Section 3 we derive algorithm for multi-agent coordinated control. In Section 4 we present a mechanism for collision avoidance. Experimental results are presented in Section 5. Conclusions are given in Section 6.

## II. Mathematical Preliminaries

Here, we recall some concepts from the control systems theory that will be used in the subsequent sections.

### A. Agent's Kinematics and Tracking Error Dynamics

We consider formation tracking of a group of $n$ unicycle agents. Kinematics of an agent $i$ ($i \in \{1,2,\dots,n\}$), depicted in Fig. 1, is described by a non-holonomic model [9-11]:

$$\begin{aligned} \dot{x}_i &= v_i \cos\theta_i, \\ \dot{y}_i &= v_i \sin\theta_i, \\ \dot{\theta}_i &= \omega_i, \end{aligned} \tag{1}$$

where $v_i$ and $\omega_i$ are the forward and steering velocities, respectively, $x_i$ and $y_i$ are the planar coordinates of the agent's midpoint $\mathrm{O}_e$ in the world coordinate frame $\mathrm{O}xy$, and $\theta_i$ is the heading angle relative to the $x$-axis of the world frame.

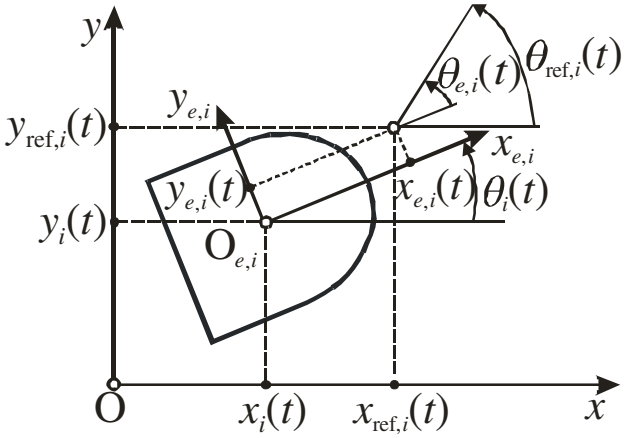


Fig. 1. Configuration and error coordinates of a unicycle agent.

The reference trajectory of the agent $i$ is given in $\mathrm{O}xy$:

$$\mathbf{p}_{\mathrm{ref},i}(t) = [x_{\mathrm{ref},i}(t) \quad y_{\mathrm{ref},i}(t) \quad \theta_{\mathrm{ref},i}(t)]^T. \tag{2}$$

Due to the non-holonomic constraint in (1), the reference Cartesian velocities and the heading angle satisfy $-\dot{x}_{\mathrm{ref},i}\sin\theta_{\mathrm{ref},i} + \dot{y}_{\mathrm{ref},i}\cos\theta_{\mathrm{ref},i} = 0$. For $\dot{x}_{\mathrm{ref},i} \neq 0$, $\dot{y}_{\mathrm{ref},i} \neq 0$, the reference forward and steering velocities are defined by

$$\begin{aligned} v_{\mathrm{ref},i} &= \sqrt{\left(\dot{x}_{\mathrm{ref},i}\right)^2 + \left(\dot{y}_{\mathrm{ref},i}\right)^2}, \\ \omega_{\mathrm{ref},i} &= \frac{\dot{x}_{\mathrm{ref},i}\ddot{y}_{\mathrm{ref},i} - \ddot{x}_{\mathrm{ref},i}\dot{y}_{\mathrm{ref},i}}{\left(v_{\mathrm{ref},i}\right)^2}. \end{aligned} \tag{3}$$

The trajectories of all the agents constitute a formation, characterized by a specific spatial pattern of the agents (e.g. platoon). This pattern may change in time.

Our goal is to design control laws for $v_i$ and $\omega_i$ in (1), $i \in \{1,2,\dots,n\}$, such that each agent asymptotically tracks its own reference $\mathbf{p}_{\mathrm{ref},i}(t)$ and the formation between the agents is achieved. If motion of any of the agents is perturbed, then controllers of interacting agents should be coordinated such as to restore the formation even at the cost of performance of tracking the individual reference trajectories.

For control design we consider tracking errors of the agent $i$, $i \in \{1,2,\dots,n\}$, represented relative to the agent's coordinate frame $\mathrm{O}_{e,i}x_{e,i}y_{e,i}$ [9-11], see Fig. 1:

$$\begin{bmatrix} x_{e,i} \\ y_{e,i} \\ \theta_{e,i} \end{bmatrix} = \begin{bmatrix} \cos\theta_i & \sin\theta_i & 0 \\ -\sin\theta_i & \cos\theta_i & 0 \\ 0 & 0 & 1 \end{bmatrix} \begin{bmatrix} x_{\mathrm{ref},i} - x_i \\ y_{\mathrm{ref},i} - y_i \\ \theta_{\mathrm{ref},i} - \theta_i \end{bmatrix}. \tag{4}$$

Dynamics of the errors $(x_{e,i}, y_{e,i}, \theta_{e,i})$ are modeled in [9]:

$$\dot{\mathbf{e}}_{xy,i} = -\mathbf{S}(\omega_i)\mathbf{e}_{xy,i} + \begin{bmatrix} v_{\mathrm{ref},i}\cos\theta_{e,i} - v_i \\ v_{\mathrm{ref},i}\sin\theta_{e,i} \end{bmatrix},$$

$$\dot{\theta}_{e,i} = \omega_{\mathrm{ref},i} - \omega_i, \tag{5a}$$

$$\mathbf{e}_{xy,i} = \begin{bmatrix} x_{e,i} \\ y_{e,i} \end{bmatrix}, \quad \mathbf{S}(\omega_i) = \begin{bmatrix} 0 & -\omega_i \\ \omega_i & 0 \end{bmatrix}. \tag{5b}$$

The skew-symmetric matrix $\mathbf{S}$ features the well-known property (7), which is used in our control design in Section 3:

$$\mathbf{x}^T\mathbf{S}\mathbf{x} \equiv 0, \ \forall \mathbf{x} \in \mathbb{R}^2. \tag{6}$$

### B. A Concept from Stability Theory

The following lemma has already been formulated in [11]. For convenience, we repeat it here again.

*Lemma 1:* Consider a scalar system:

$$\dot{x}(t) = -\phi(x(t)) + p(t), \tag{7}$$

where $\phi$ and $p$ are bounded and uniformly continuous functions of $x$ and $t$, respectively, such that $\phi(0) = 0$ and $x\phi(x) > 0$ if $x \neq 0$. If, for any $t_0 \geq 0$ and any initial condition $x(t_0)$, the solution $x(t)$ is bounded and $\lim_{t\to\infty} x(t) = 0$, then

$$\lim_{t\to\infty} p(t) = 0. \tag{8}$$

*Proof*: See [11]. ■

### C. Saturation Functions

For the sake of control design, we need to introduce a set of saturation functions in a similar way as in [11]. A class $\mathrm{BF}_{r,k}$ of uniformly continuous and bounded functions indexed by (possibly time-variant) bounded parameters $r, k \in \mathrm{R}_+$ is defined as:

Preprint submitted to 2010 American Control Conference.
Received September 28, 2009.

$$\mathrm{BF}_{r,k} = \{\phi_r(kx):\mathrm{R} \to \mathrm{R} \mid \phi_r(kx) \text{ is uniformly continuous and } -r \le \phi_r(kx) \le r \ \ \forall x \in \mathrm{R}\}. \quad (9)$$

Within this class, we consider a set $\mathrm{S}_{r,k}$ of odd functions:

$$\mathrm{S}_{r,k} = \{\phi_r(kx):\mathrm{R} \to \mathrm{R} \mid \phi_r(kx) \in \mathrm{BF}_{r,k}, \phi_r(0) \equiv 0, x\phi_r(kx) > 0 \text{ for all } x \neq 0, \phi_r(kx) + \phi_r(-kx) \equiv 0\}. \quad (10)$$

Examples of nontrivial, yet simple, functions in $\mathrm{S}_{r,k}$ are:

$$\phi_r(kx) = r\frac{kx}{\sqrt{1+(kx)^2}}, \quad (11a)$$

$$\phi_r(kx) = r\tanh(kx). \quad (11b)$$

## III. Control Design

In this section we will derive tracking control laws $v_i$ and $\omega_i$, $i \in \{1,2,\dots,n\}$, such as to achieve motion coordination of $n$ interacting agents. This derivation will conceptually mimic the approach followed in [10,11]. The position errors, defined by (4) and (5b), of all agents are put in two vectors:

$$\mathbf{e}_{xy} = \left[\left(\mathbf{e}_{xy,1}\right)^T, \dots, \left(\mathbf{e}_{xy,n}\right)^T\right]^T, \ \boldsymbol{\theta}_e = \left[\theta_{e,1}, \dots, \theta_{e,n}\right]^T. \quad (12)$$

We design time-varying state-feedback control laws

$$v_i = v_i^*\left(t, \mathbf{e}_{xy}, \boldsymbol{\theta}_e\right), \ \omega_i = \omega_i^*\left(t, \mathbf{e}_{xy}, \boldsymbol{\theta}_e\right), \quad (13)$$

for $i \in \{1,2,\dots,n\}$, such as to ensure global asymptotic stability of the error dynamics (5a) under constraints

$$|v_i(t)| \le v_{\max,i}, \ \ |\omega_i(t)| \le \omega_{\max,i}, \ \ \forall t \ge 0. \quad (14)$$

Here, $v_{\max,i}$ and $\omega_{\max,i}$ are given positive constants.

The following controller solves the given problem:

$$v_i(t) = v_{\mathrm{ref},i}(t)\cos\theta_{e,i} + \phi_{k_{x,i}(t)}\left(c_{x,i}x_{e,i}\right) + \sum_{\substack{j=1 \\ j\neq i}}^{n} \frac{l_{xx,i,j}(t)x_{e,j}\phi_{k_{xx,i,j}(t)}\left(c_{xx,i,j}\left(x_{e,i}-x_{e,j}\right)\right)}{\sqrt{1+\left(l_{xx,i,j}(t)x_{e,i}x_{e,j}\right)^2}}, \quad (15a)$$

$$\omega_i(t) = \omega_{\mathrm{ref},i}(t) + \phi_{k_{\theta,i}(t)}\left(c_{\theta,i}\theta_{e,i}\right) + \frac{ky_{e,i}k_y v_{\mathrm{ref},i}(t)}{\sqrt{1+k^2\left(\mathbf{e}_{xy}\right)^T\mathbf{e}_{xy}}}\frac{\sin\theta_{e,i}}{\theta_{e,i}} + \sum_{\substack{j=1 \\ j\neq i}}^{n}\left(\frac{l_{\theta\theta,i,j}(t)\theta_{e,j}\phi_{k_{\theta\theta,i,j}(t)}\left(c_{\theta\theta,i,j}\left(\theta_{e,i}-\theta_{e,j}\right)\right)}{\sqrt{1+\left(l_{\theta\theta,i,j}(t)\theta_{e,i}\theta_{e,j}\right)^2}} + \phi_{k_{yy,i,j}(t)}\left(c_{yy,i,j}\left(y_{e,i}-y_{e,j}\right)\right)\frac{\sin\theta_{e,i}}{\theta_{e,i}}\sin\theta_{e,j}\right), \quad (15b)$$

where $k_{x,i}(t), k_{\theta,i}(t), c_{x,i}, c_{\theta,i}, k_y, k, k_{a,i,j}(t), c_{a,i,j}, l_{a,i,j}(t)$ are the design parameters with $a \in \{xx, \theta\theta, yy\}$, and $\phi_{k_{x,i}}(c_{x,i}x)$, $\phi_{k_{\theta,i}}(c_{\theta,i}\theta)$ and $\phi_{k_{a,i,j}(t)}\left(c_{a,i,j}x\right)$ are the saturation functions from the sets $\mathrm{S}_{k_{x,i},c_{x,i}}$, $\mathrm{S}_{k_{\theta,i},c_{\theta,i}}$ and $\mathrm{S}_{k_{a,i,j},c_{a,i,j}}$ defined by (10), respectively. The design parameters that can be chosen as time-variant have explicit time-arguments in (15a,b). Note that

$$\frac{\sin\theta_{e,i}}{\theta_{e,i}} = \int_0^1 \cos(s\theta_{e,i})\mathrm{d}s \quad (16)$$

is a smooth function in $\theta_{e,i}$ and recall that

$$\lim_{\theta_{e,i}\to 0}\frac{\sin\theta_{e,i}}{\theta_{e,i}} = 1. \quad (17)$$

We establish the following result.

*Theorem 1*: Consider a group of $n$ unicycle agents. Kinematics of an agent $i$, $i \in \{1,2,\dots,n\}$, are described by (1). The inputs $v_i$ and $\omega_i$ are constrained according to (14). Assume that the desired trajectory in (2) meets the constraints $\left|v_{\mathrm{ref},i}(t)\right| < v_{\max,i}$, $\left|\omega_{\mathrm{ref},i}(t)\right| < \omega_{\max,i}$, $\forall t \ge 0$, and the trajectories of all the agents constitute a formation. The tracking error dynamics of an agent $i$ are given by (5), and the error vectors are defined by (12). Introduce symbol $a$ such as $a \in \{xx, \theta\theta, yy\}$, and consider the controller (15) in 2 cases that depend on properties of the reference velocities.

1. Suppose that for all $i \in \{1,2,\dots,n\}$ over $t \in [0,\infty)$, $v_{\mathrm{ref},i}(t)$ is nonzero, bounded and uniformly continuous, while $\omega_{\mathrm{ref},i}(t)$ is just bounded. If the design parameters in (15) are chosen such that

$$k_{x,i}(t), k_{\theta,i}(t), c_{x,i}, c_{\theta,i}, k_y, k \in \mathbb{R}_+ \quad (18a)$$

$$k_{a,i,j}(t), c_{a,i,j}, l_{a,i,j}(t) \in \mathbb{R}_+ \cup \{0\} \quad (18b)$$

$$k_{a,i,j}(t) \equiv k_{a,j,i}(t) \quad (18c)$$

$$c_{a,i,j} = c_{a,j,i} \quad (18d)$$

$$l_{a,i,j}(t) \equiv l_{a,j,i}(t) \quad (18e)$$

$$k_{x,i}(t) + \sum_{\substack{j=1 \\ j\neq i}}^{n} k_{xx,i,j}(t) \le v_{\max,i} - \left|v_{\mathrm{ref},i}(t)\right|, \quad (18f)$$

$$k_{\theta,i}(t) + k_y\left|v_{\mathrm{ref},i}(t)\right| + \sum_{\substack{j=1 \\ j\neq i}}^{n}\left(k_{\theta\theta,i,j}(t) + k_{yy,i,j}(t)\right) \le \omega_{\max,i} - \left|\omega_{\mathrm{ref},i}(t)\right| \quad (18g)$$

then $\left(\mathbf{e}_{xy}, \boldsymbol{\theta}_e\right) = \mathbf{0}$ is a globally asymptotically stable equilibrium of the tracking error dynamics.

2. Suppose that for all $i \in \{1,2,\dots,n\}$ over $t \in [0,\infty)$, $v_{\mathrm{ref},i}(t)$ is bounded, uniformly continuous and for some $i$ it converges to zero as $t \to \infty$, while every $\omega_{\mathrm{ref},i}(t)$ is nonzero, bounded and uniformly continuous. If the design parameters are chosen as in (18), then $\left(\mathbf{e}_{xy}, \boldsymbol{\theta}_e\right) = \mathbf{0}$ is a globally asymptotically stable equilibrium of the tracking error dynamics.

*Proof*: Consider the positive definite and proper Lyapunov function candidate $V\left(\mathbf{e}_{xy}, \boldsymbol{\theta}_e\right)$:

$$V = \frac{k_y}{k}\sqrt{1+k^2\left(\mathbf{e}_{xy}\right)^T\mathbf{e}_{xy}} + 0.5(\boldsymbol{\theta}_e)^T\boldsymbol{\theta}_e - \frac{k_y}{k}, \quad (19)$$

where $k_y, k \in \mathbb{R}_+$ are constant design parameters. Differentiating $V$ along the solutions of the closed-loop system (5),(15) with $i \in \{1,2,\dots,n\}$ yields

$$\frac{\mathrm{d}}{\mathrm{d}t}V\left(\mathbf{e}_{xy}, \boldsymbol{\theta}_e\right) = \frac{k_y k\left(\mathbf{e}_{xy}\right)^T\dot{\mathbf{e}}_{xy}}{\sqrt{1+k^2\left(\mathbf{e}_{xy}\right)^T\mathbf{e}_{xy}}} + \boldsymbol{\theta}_e\dot{\boldsymbol{\theta}}_e$$

$$= \frac{k_y k}{\sqrt{1+k^2\left(\mathbf{e}_{xy}\right)^T\mathbf{e}_{xy}}}\left(-\left(\mathbf{e}_{xy}\right)^T\begin{bmatrix}\mathbf{S}(\omega_1) & \cdots & \mathbf{0}_{2\times 2} \\ \vdots & \ddots & \vdots \\ \mathbf{0}_{2\times 2} & \cdots & \mathbf{S}(\omega_n)\end{bmatrix}\mathbf{e}_{xy} + \right.$$

Preprint submitted to 2010 American Control Conference.
Received September 28, 2009.

$$\left(\mathbf{e}_{xy}\right)^T\begin{bmatrix} v_{\mathrm{ref},1}\cos\theta_{e,1}-v_1 \\ v_{\mathrm{ref},1}\sin\theta_{e,1} \\ \vdots \\ v_{\mathrm{ref},n}\cos\theta_{e,n}-v_n(t) \\ v_{\mathrm{ref},n}\sin\theta_{e,n}\end{bmatrix}\Bigg) + \sum_{i=1}^{n}\left[\theta_{e,i}\left(\omega_{\mathrm{ref},i}-\omega_i\right)\right]$$

$$= \frac{k_y k\sum_{i=1}^{n}\left[-x_{e,i}\phi_{k_{x,i}(t)}\left(c_{x,i}x_{e,i}\right)+y_{e,i}v_{\mathrm{ref},i}\sin\theta_{e,i}\right]}{\sqrt{1+k^2\left(\mathbf{e}_{xy}\right)^T\mathbf{e}_{xy}}}$$

$$-\sum_{i=1}^{n}\left[\theta_{e,i}\phi_{k_{\theta,i}(t)}\left(c_{\theta,i}\theta_{e,i}\right)\right]-\frac{k_y k\sum_{i=1}^{n}\left[y_{e,i}v_{\mathrm{ref},i}\sin\theta_{e,i}\right]}{\sqrt{1+k^2\left(\mathbf{e}_{xy}\right)^T\mathbf{e}_{xy}}}$$

$$-\frac{k_y k}{\sqrt{1+k^2\left(\mathbf{e}_{xy}\right)^T\mathbf{e}_{xy}}}A_x - A_\theta - A_y$$

$$= \frac{-k_y k\sum_{i=1}^{n}\left[x_{e,i}\phi_{k_{x,i}(t)}\left(c_{x,i}x_{e,i}\right)\right]}{\sqrt{1+k^2\left(\mathbf{e}_{xy}\right)^T\mathbf{e}_{xy}}}$$

$$-\sum_{i=1}^{n}\left[\theta_{e,i}\phi_{k_{\theta,i}(t)}\left(c_{\theta,i}\theta_{e,i}\right)\right]\le 0. \qquad (20)$$

In (20), $A_x$ and $A_\theta$ have form of

$$A_b = \sum_{i=1}^{n}\sum_{\substack{j=1\\ j\neq i}}^{n}\frac{l_{bb,i,j}(t)b_{e,i}b_{e,j}\phi_{k_{bb,i,j}(t)}\left(c_{bb,i,j}\left(b_{e,i}-b_{e,j}\right)\right)}{\sqrt{1+\left(l_{bb,i,j}(t)b_{e,i}b_{e,j}\right)^2}}$$

$$= \sum_{i=1}^{n-1}\sum_{j=i+1}^{n}\Bigg\{\frac{l_{bb,i,j}(t)b_{e,i}b_{e,j}}{\sqrt{1+\left(l_{bb,i,j}(t)b_{e,i}b_{e,j}\right)^2}}$$

$$\left[\phi_{k_{bb,i,j}(t)}\left(c_{bb,i,j}\left(b_{e,i}-b_{e,j}\right)\right)+\phi_{k_{bb,i,j}(t)}\left(c_{bb,i,j}\left(b_{e,j}-b_{e,i}\right)\right)\right]\Bigg\}$$

$$=0, \qquad (21)$$

with $b\in\{x,\theta\}$, while

$$A_y = \sum_{i=1}^{n}\sum_{\substack{j=1\\ j\neq i}}^{n}\left[\phi_{k_{yy,i,j}(t)}\left(c_{yy,i,j}\left(y_{e,i}-y_{e,j}\right)\right)\sin\theta_{e,i}\sin\theta_{e,j}\right]$$

$$= \sum_{i=1}^{n-1}\sum_{j=i+1}^{n}\Big\{\sin\theta_{e,i}\sin\theta_{e,j}\left[\phi_{k_{yy,i,j}(t)}\left(c_{yy,i,j}\left(y_{e,i}-y_{e,j}\right)\right)+\phi_{k_{yy,i,j}(t)}\left(c_{yy,i,j}\left(y_{e,j}-y_{e,i}\right)\right)\right]\Big\}$$

$$=0, \qquad (22)$$

The last equalities in (21) and (22) stem from the fact that $\phi_r(kx)$ is an odd function, see the definition (10).

We use the property (6) to obtain the expression given in the third row of (20). The last inequality in (20), which follows from the properties of functions from the set defined by (10), implies that the trajectories of the tracking errors $x_{e,i}(t)$, $y_{e,i}(t)$ and $\theta_{e,i}(t)$, $i\in\{1,2,\dots,n\}$, are uniformly bounded over $t\in[0,\infty)$. It remains to show global asymptotic convergence of these errors to $\left(\mathbf{e}_{xy},\boldsymbol{\theta}_e\right)=\mathbf{0}$.

From the last inequality in (20) we can determine

$$0\ge\int_0^\infty \mathrm{d}V(t)\ge -\sum_{i=1}^{n}\Big\{\int_0^\infty x_{e,i}(t)\phi_{k_{x,i}(t)}\left(c_{x,i}x_{e,i}(t)\right)\mathrm{d}t + \int_0^\infty\theta_{e,i}(t)\phi_{k_{\theta,i}(t)}\left(c_{\theta,i}\theta_{e,i}(t)\right)\mathrm{d}t\Big\}, \qquad (23)$$

which implies that the integrals at the right hand side in (23) exist and are finite. Having in mind that by definition (10) $x_{e,i}(t)\phi_{k_{x,i}(t)}\left(c_{x,i}x_{e,i}(t)\right)$ and $\theta_{e,i}(t)\phi_{k_{\theta,i}(t)}\left(c_{\theta,i}\theta_{e,i}(t)\right)$ are non-negative, then for all $i\in\{1,2,\dots,n\}$ we have $x_{e,i}\phi_{k_{x,i}(t)}\left(c_{x,i}x_{e,i}\right),\phi_{k_{\theta,i}(t)}\left(c_{\theta,i}\theta_{e,i}\right)\in L_1(0,\infty)$. Since both $x_{e,i}(t)\phi_{k_{x,i}(t)}\left(c_{x,i}x_{e,i}(t)\right)$, $\theta_{e,i}(t)\phi_{k_{\theta,i}(t)}\left(c_{\theta,i}\theta_{e,i}(t)\right)$ are by assumption uniformly continuous over $t\in[0,\infty)$, while $x_{e,i}$ and $\theta_{e,i}$ are solutions of the continuous error dynamics (5) which is excited with inputs (15a,b) made of the uniformly continuous functions and bounded $v_{\mathrm{ref},i}(t)$ and $\omega_{\mathrm{ref},i}(t)$, then all $x_{e,i}(t)\phi_{k_{x,i}(t)}\left(c_{x,i}x_{e,i}(t)\right)$ and $\theta_{e,i}(t)\phi_{k_{\theta,i}(t)}\left(c_{\theta,i}\theta_{e,i}(t)\right)$ must be uniformly continuous over $t\in[0,\infty)$. With the help of Barbălat's lemma [13] (pp. 211), we get

$$\lim_{t\to\infty}\sum_{i=1}^{n}\Big[x_{e,i}(t)\phi_{k_{x,i}(t)}\left(c_{x,i}x_{e,i}(t)\right)+\theta_{e,i}(t)\phi_{k_{\theta,i}(t)}\left(c_{\theta,i}\theta_{e,i}(t)\right)\Big]=0, \qquad (24)$$

implying

$$\lim_{t\to\infty}\left[\left|x_{e,i}(t)\right|+\left|\theta_{e,i}(t)\right|\right]=0,\ \forall i\in\{1,2,\dots,n\}. \qquad (25)$$

It remains to prove

$$\lim_{t\to\infty}y_{e,i}(t)=0,\ \forall i\in\{1,2,\dots,n\}. \qquad (26)$$

First we consider the case when every $v_{\mathrm{ref},i}(t)$ remains nonzero. From the closed-loop system (5),(15) we obtain:

$$\dot\theta_{e,i}(t)=-\phi_{k_{\theta,i}(t)}\left(c_{\theta,i}\theta_{e,i}\right)-\frac{k y_{e,i}k_y v_{\mathrm{ref},i}(t)}{\sqrt{1+k^2\left(\mathbf{e}_{xy}\right)^T\mathbf{e}_{xy}}}\frac{\sin\theta_{e,i}}{\theta_{e,i}}$$

$$-\sum_{\substack{j=1\\ j\neq i}}^{n}\left(\frac{l_{\theta\theta,i,j}(t)\theta_{e,j}\phi_{k_{\theta\theta,i,j}(t)}\left(c_{\theta\theta,i,j}\left(\theta_{e,i}-\theta_{e,j}\right)\right)}{\sqrt{1+\left(l_{\theta\theta,i,j}(t)\theta_{e,i}\theta_{e,j}\right)^2}}+\phi_{k_{yy,i,j}(t)}\left(c_{yy,i,j}\left(y_{e,i}-y_{e,j}\right)\right)\frac{\sin\theta_{e,i}}{\theta_{e,i}}\sin\theta_{e,j}\right). \qquad (27)$$

A direct application of the Lemma 1 to (27) results in:

$$\lim_{t\to\infty}\left(\frac{k y_{e,i}k_y v_{\mathrm{ref},i}(t)}{\sqrt{1+k^2\left(\mathbf{e}_{xy}\right)^T\mathbf{e}_{xy}}}\frac{\sin\theta_{e,i}}{\theta_{e,i}}\right)=0. \qquad (28)$$

Having in mind (17),(25), and that $v_{\mathrm{ref},i}(t)$ remains nonzero, property (26) must hold. Note that the expression (27) does not depend on the steering velocities. Consequently, global asymptotic stability of the tracking error dynamics does not require uniform continuity of these velocities.

In the second case, where it is assumed that for some $i$ we have $\lim_{t\to\infty}v_{\mathrm{ref},i}(t)=0$ while every $\omega_{\mathrm{ref},i}(t)$ remains nonzero, one should consider the $x_e$ equation of the closed-loop system (5),(15). The proof proceeds similarly as in the first case and can therefore be omitted. A notable difference is that the application of Lemma 1 on the $x_e$ equation does demand uniform continuity of $\omega_{\mathrm{ref},i}(t)$.

Selection of the design parameters according to (18f,g) trivially ensures that the control inputs (15a,b) fulfill (14). ■

Preprint submitted to 2010 American Control Conference.
Received September 28, 2009.

*Remark*: According to (18b), the design parameters appearing in the coupling terms of the control laws (15a,b) must be nonnegative. If the individual agents suffer from perturbations, by means of strictly positive coupling gains the controller (15a,b) mediates between tracking of the reference trajectories of the individual agents and keeping the formation between the agents. The coordination between some agents can be switched off (even online) by assigning zero values to the corresponding coupling gains.

The design parameters in (15) offer high freedom in tuning the transient behavior of the closed-loop system: we can speed-up correction of the tracking errors and adjust robustness of the formation to perturbations. By means of the time-varying design parameters, we can online influence the tracking performance, on one hand, and strengthen or loosen couplings between individual agents, on another. For instance, without violating the constraints (15), we can allow high-gain feedback during periods of slower movements. Increased feedback gains can improve tracking performance at low velocities, especially if an agent is subject to parasitic dynamics and disturbances (e.g., friction on the robot wheels, noise in the feedback signals). On the other hand, larger coupling gains $k_{xx,i,j}$, $k_{\theta\theta,i,j}$ and $k_{yy,i,j}$ in (15) increase interaction among the agents and improve robustness of the formation against perturbations on any agent. This will be illustrated in a case-study in Section 5.

As the last merit of our control design, we point out that $\omega_{\mathrm{ref},i}(t)$ needs not to be uniformly continuous if $v_{\mathrm{ref},i}(t)$ is nonzero. Hence, the global asymptotic stability of the tracking error dynamics is ensured even if $\omega_{\mathrm{ref},i}(t)$ is discontinuous (yet bounded). This is very relevant for motion coordination along trajectories consisting of straight and curved segments. At blending points between the straight- and curved-parts, the steering velocities of the individual agents may become discontinuous, especially if their forward velocities must remain constant. Despite eventual discontinuities in $\omega_{\mathrm{ref},i}(t)$, the control laws (15a,b) guarantee globally asymptotic convergence of the tracking errors.

## IV. A Method for Collision Avoidance

To benefit from motion coordination using the controller derived in Section 3 in practical applications, it is necessary to ensure real-time inter-agent and agent-obstacle collision avoidance. Therefore, we enhance the control design with an online Artificial Potential Field (APF) strategy [12]. An APF is designed for each agent locally, and it tends high when an agent approaches the boundary of a pre-given safety area. Based on position information about obstacles and the other agents, the local algorithm of an agent modifies the agent's reference trajectory in real-time as soon as an obstructor (obstacle or another agent) enters the detection region. The reference trajectory is modified such as to ensure collision-free movements. In this section, we will present our method for collision avoidance of the agents only. The same method applies for collision avoidance with obstacles.

An APF of agent $i$, $i \in \{1,2,\dots,n\}$, may have the form:

$$V_i = \sum_{\substack{j=1 \\ j\neq i}}^{n} V_{i,j}(x_i - x_j, y_i - y_j), \tag{29}$$

where

$$V_{i,j}(x_i - x_j, y_i - y_j) = K_{\mathrm{a},i}\left[(x_i - x_{\mathrm{ref},i})^2 + (y_i - y_{\mathrm{ref},i})^2\right] + K_{\mathrm{o},i} e^{-\frac{1}{p}\left[\left(\frac{x_i - x_j}{\alpha}\right)^p + \left(\frac{y_i - y_j}{\beta}\right)^p\right]} \text{ if } \left(\frac{x_i - x_j}{\alpha}\right)^p + \left(\frac{y_i - y_j}{\beta}\right)^p \leq 1,$$
$$V_{i,j}(x_i - x_j, y_i - y_j) = 0 \text{ if } \left(\frac{x_i - x_j}{\alpha}\right)^p + \left(\frac{y_i - y_j}{\beta}\right)^p > 1. \tag{30}$$

Here, $(x_i, y_i)$ and $(x_j, y_j)$ are the Cartesian coordinates of the agents $i$ and $j$, respectively, $K_{\mathrm{a},i}$ and $K_{\mathrm{o},i}$ are the gains of the attractive and repulsive components of the potential $V_{i,j}$, respectively, while the real numbers $\alpha$ and $\beta$ and the integer $p$ are the positive parameters influencing size and shape of the safety-area. The higher the positive integer $p$ is, the shape of the safety area is more rectangular alike. Based on (30), $V_{i,j}$ takes zero value outside the detection region of the agent $i$. Inside this region, the reference trajectory of the agent $i$ is online modified according to the following algorithm.

Step 1: Determine Cartesian velocities that move the agent away of the obstructor due to the repulsive potential:

$$\begin{bmatrix} \delta v'_{x,i} \\ \delta v'_{y,i} \end{bmatrix} = -\begin{bmatrix} \frac{\partial V_i}{\partial x_i} \\ \frac{\partial V_i}{\partial y_i} \end{bmatrix}, \tag{31}$$

$$\delta v_i = \sqrt{\left(\delta v'_{x,i}\right)^2 + \left(\delta v'_{y,i}\right)^2}, \tag{32}$$

Step 2: Adjust the velocities determined in the previous step such as to meet the constraint (14):

$$\begin{bmatrix} \delta v_{x,i} \\ \delta v_{y,i} \end{bmatrix} = \begin{cases} \frac{v_{\max,i}}{\delta v_i}\begin{bmatrix} \delta v'_{x,i} \\ \delta v'_{y,i} \end{bmatrix}, & \text{if } \delta v_i > v_{\max,i}, \\ \begin{bmatrix} \delta v'_{x,i} \\ \delta v'_{y,i} \end{bmatrix}, & \text{otherwise.} \end{cases} \tag{33}$$

Step 3: Find the collision-free trajectories at time-instant $t_k$:

$$x_{\mathrm{ref},i}(t_k) = x_i(t_{k-1}) + (t_k - t_{k-1})\,\delta v_{x,i}, \tag{34a}$$
$$y_{\mathrm{ref},i}(t_k) = y_i(t_{k-1}) + (t_k - t_{k-1})\delta v_{y,i}, \tag{34b}$$
$$\theta_{\mathrm{ref},i}(t_k) = \begin{cases} \operatorname{atan}(\delta v_{y,i}/\delta v_{x,i}), & \delta v_i > 0, \\ \theta_{\mathrm{ref},i}(t_{k-1}), & \delta v_i = 0, \end{cases} \tag{34c}$$
$$v_{\mathrm{ref},i}(t_k) = \sqrt{\left(\delta v_{x,i}\right)^2 + \left(\delta v_{y,i}\right)^2}, \tag{34d}$$
$$\omega_{\mathrm{ref},i}(t_k) = \left(\theta_{\mathrm{ref},i}(t_k) - \theta_{\mathrm{ref},i}(t_{k-1})\right)/(t_k - t_{k-1}). \tag{34e}$$

The proposed algorithm for collision avoidance does not hamper stability of the closed-loop system (5),(15), since this algorithm only modifies the reference trajectories of the agents facing collisions. Despite modifications, the reference motions remain continuous. Since the control law (15a,b) is also used to realize the modified trajectories, stability must hold for the modified trajectories, as well, as according to the proof of the Theorem 1, for all $i \in \{1,2,\dots,n\}$ the tracking errors $x_{e,i}$, $y_{e,i}$ and $\theta_{e,i}$ are uniformly bounded over $t \in [0,\infty)$. However, inside the detection region of the agent $i$ we cannot guarantee asymptotic tracking of the reference

Preprint submitted to 2010 American Control Conference.
Received September 28, 2009.

trajectories generated using the algorithm presented above under all circumstances, since we cannot ensure the requirement of the Theorem 1 on uniform continuity of $\omega_{\mathrm{ref},i}$ when $v_{\mathrm{ref},i}$ becomes zero. Eventual lack of the asymptotic stability may degrade performance of the collision avoidance algorithm, since effectiveness of this algorithm obviously depends on accuracy of tracking of the reference trajectory (34a-e). A pragmatic way to tackle this issue is to increase the size of the safety region. In this way we can enforce the agent $i$ to earlier respond to the threat of collision, which may practically give it sufficient space for collision-fee movements despite eventual errors in tracking the trajectory (34).

## V. Experimental Case-study

To illustrate the results presented so far, we conduct experiments on the setup depicted in Fig. 2, consisting of four mobile robots (model E-puck [13]), a camera as localization device, and a PC. The PC generates robot trajectories, processes camera images to determine actual linear and angular coordinates of each robot, and runs algorithms for formation control and obstacle avoidance. The algorithms for coordinated motion control and obstacle avoidance are not implemented locally on the robots due to limiting processing power of their onboard processors. The PC executes the algorithms for each robot separately, as these would run on the individual units. The PC sends the control inputs (forward and steering velocity commands) to the robots via BlueTooth protocol.

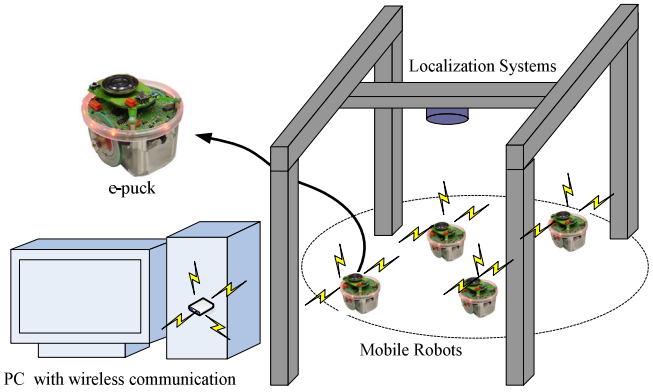


Fig. 2. The main components of the experimental setup.

Each robot is supposed to track its own reference trajectory $\mathbf{p}_{\mathrm{ref},i}(t)$, $i \in \{1,2,3,4\}$. The reference trajectories form a platoon-like spatial formation. The platoon makes a round trip. In Figure 3, the reference paths of the individual robots belonging to the platoon are depicted with the solid lines. The prescribed spatial pattern of the platoon-like formation can be characterized in terms of time-varying Euclidean distances between the neighboring robots $\Delta_{\mathrm{ref},i,j}(t)$:

$$\begin{bmatrix}\Delta_{\mathrm{ref},1,2}(t)\\ \Delta_{\mathrm{ref},2,3}(t)\\ \Delta_{\mathrm{ref},3,4}(t)\end{bmatrix} = \begin{bmatrix}\sqrt{\left(x_{\mathrm{ref},1}(t)-x_{\mathrm{ref},2}(t)\right)^2+\left(y_{\mathrm{ref},1}(t)-y_{\mathrm{ref},2}(t)\right)^2}\\ \sqrt{\left(x_{\mathrm{ref},2}(t)-x_{\mathrm{ref},3}(t)\right)^2+\left(y_{\mathrm{ref},2}(t)-y_{\mathrm{ref},3}(t)\right)^2}\\ \sqrt{\left(x_{\mathrm{ref},3}(t)-x_{\mathrm{ref},4}(t)\right)^2+\left(y_{\mathrm{ref},3}(t)-y_{\mathrm{ref},4}(t)\right)^2}\end{bmatrix}. \quad (35)$$

The Euclidean distances are actually constant (12 cm) if all four robots move along the straight-line segments of the reference paths and decrease continuously (minimum of 11.5 cm) on the circular corners of these paths.

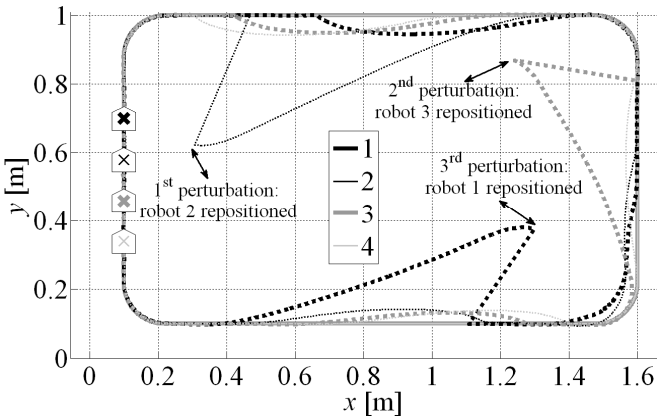


Fig. 3. Reference (solid) and actual (dotted) robot paths in the experiment; the initial and terminal positions are coinciding and are indicated with '×'.

We use the following tracking controllers, $i \in \{1,2,3,4\}$:

$$\begin{aligned} v_i(t) = {} & v_{\mathrm{ref},i}(t)\cos\theta_{e,i} \\ & +\left(v_{\max}-\left|v_{\mathrm{ref},i}(t)\right|-3k_{xx}\right)\tanh\left(20x_{e,i}(t)\right) \\ & +k_{xx}\sum_{\substack{j=1\\ j\neq i}}^{4}\frac{100x_{e,j}\tanh\left(1.5\left(x_{e,i}-x_{e,j}\right)\right)}{\sqrt{1+\left(100x_{e,i}x_{e,j}\right)^2}}, \end{aligned} \quad (36a)$$

$$\begin{aligned} \omega_i(t) = {} & \omega_{\mathrm{ref},i}(t) + \\ & \frac{11v_{\mathrm{ref},i}(t)200y_{e,i}(t)}{\sqrt{1+200^2\sum_{i=1}^{4}\left[\left(x_{e,i}(t)\right)^2+\left(y_{e,i}(t)\right)^2\right]}}\,\frac{\sin\left(\theta_{e,i}(t)\right)}{\theta_e(t)} \\ & +\left(\omega_{\max}-\left|\omega_{\mathrm{ref},i}(t)\right|-11\left|v_{\mathrm{ref},i}(t)\right|\right. \\ & \left.-3k_{\theta\theta}-3k_{yy}\right)\tanh\left(\theta_{e,i}(t)\right) \\ & +k_{\theta\theta}\sum_{\substack{j=1\\ j\neq i}}^{4}\frac{100\theta_{e,j}\tanh\left(0.04\left(\theta_{e,i}-\theta_{e,j}\right)\right)}{\sqrt{1+\left(100\theta_{e,i}\theta_{e,j}\right)^2}} \\ & +k_{yy}\sum_{\substack{j=1\\ j\neq i}}^{4}\left(\tanh\left(1.5\left(y_{e,i}-y_{e,j}\right)\right)\frac{\sin\theta_{e,i}}{\theta_{e,i}}\sin\theta_{e,j}\right). \end{aligned} \quad (36b)$$

Here, $v_{\max}=0.1$ [m/s] and $\omega_{\max}=1.7$ [rad/s] are the maximum values of the control signals. Controllers (36a,b) have time-varying feedback gains $v_{\max}-\left|v_{\mathrm{ref},i}(t)\right|-3k_{xx}$ and $\omega_{\max}-\left|\omega_{\mathrm{ref},i}(t)\right|-11\left|v_{\mathrm{ref},i}(t)\right|-3k_{\theta\theta}-3k_{yy}$. Such gains increase at lower velocities, which improves robustness against disturbances and parasitic dynamics. Time-variations of the feedback gains do not hamper constraints (14), since by design both controllers are saturated. Other gains are kept constant for simplicity. The design parameters in (36a,b) are tuned to demonstrate that in the absence of

Preprint submitted to 2010 American Control Conference.
Received September 28, 2009.

perturbations four robots asymptotically track their own reference trajectories, while, if subject to perturbations, the robots prefer to maintain their formation at the cost of tracking accuracy of their individual reference trajectories. The emphasis on formation keeping is achieved by relatively strong coupling coefficients $k_{xx} = 0.008$, $k_{\theta\theta} = 0.025$ and $k_{yy} = 0.08$. In our experiment, the controller (36) is applied at a sampling rate of 25 [Hz].

To practically verify formation keeping, during the experiment we manually perturb the robot formation three times, by repositioning of the robots 2, 3 and 1 at time instants 18 s, 46 s and 65 s, respectively. The actual robot paths are depicted in Fig. 3 by the dotted line. The robots 2 and 1 are perturbed at the horizontal sections of the reference path, while the robot 3 is perturbed at the vertical section. Each time some robot is repositioned, the other ones start moving away from their reference trajectories aiming to restore the prescribed formation (35). After recovering the formation, the robots continue tracking their own reference trajectories. As an illustration, in Fig. 4 we show the tracking errors $e_{x,i} = x_{\mathrm{ref},i} - x_i$, $e_{y,i} = y_{\mathrm{ref},i} - y_i$ and $e_{\theta,i} = \theta_{\mathrm{ref},i} - \theta_i$ together with errors in keeping the formation:

$$\delta_{i,j} = \Delta_{\mathrm{ref},i,j} - \Delta_{i,j}, \qquad (37)$$

where $\Delta_{\mathrm{ref},i,j}$ and $\Delta_{i,j}$ are the reference and actual Euclidean distances between the neighboring robots, respectively.

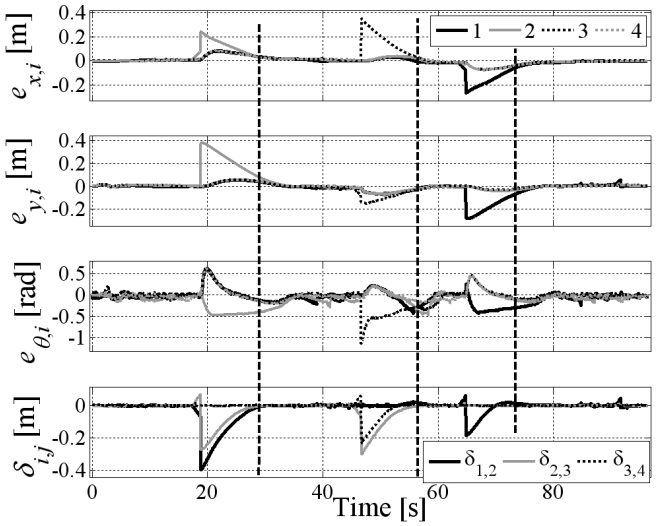


Fig. 4. Experimentally measured tracking errors ($e_{x,i}$, $e_{y,i}$ $e_{\theta,i}$) and errors in keeping the formation $\delta_{i,j}$; the vertical dashed lines identify finishing of transients of the formation errors.

A closer inspection of Fig. 4 confirms that the transients of the formation errors are faster than the transients of the tracking errors. In other words, after perturbations the robots first restore their prescribed formation and then converge to their reference trajectories. This is an experimental demonstration of robust formation keeping in the presence of perturbations. The robustness is gained by introducing the mutual coupling terms in the control law derived in Section 3.Tuning of these gains is quite intuitive: higher values are needed if keeping the formation is of higher priority; lower gains apply when it is more important to track the reference trajectories of the individual robots .

Because of the limiting space, we present no experimental data to illustrate effects of the collision avoidance algorithm formulated in Section 4. We only report that application of this algorithm results in collision-free robot motions in different experimental case-studies, including the one described in this section.

## VI. Conclusions

In this paper, we contribute a Lyapunov based design of saturated state-feedback controllers that achieve global asymptotic stability of the tracking error dynamics for multi-agent unicycle systems. The proposed design enables motion coordination of the agents such as to keep them within time-varying formation. During coordination, the forward and steering velocities of the individual agents can all be mutually different, while the steering velocities can even be discontinuous. The available control parameters allow online regulation of level of interaction among individual agents and intuitive adjustment of robustness of the formation with respect to perturbations. To further enhance robustness to perturbations, we formulate an algorithm for online collision avoidance. Experimental results demonstrate practical applicability of our contributions.

## References

[1] T. Arai, E. Pagello, L.E. Parker, "Editorial: Advances in Multi-Robot Systems," *IEEE Trans. Robot. Autom*., Vol. 18, No. 5, pp. 655-661, Oct. 2002.

[2] K.Y. Pettersen, J.T. Gravdahl, H. Nijmeijer, Eds. *Group Coordination and Cooperative Control*. Springer-Verlag, London, 2006.

[3] Y.Q. Chen, Z. Wang, "Formation Control: a Review and a New Consideration," *Proc. IEEE/RSJ Int. Conf. Int. Robots and Systems*, pp. 3181-3186, Alberta, Canada, 2005.

[4] H. Moneva, J. Caarls, J. Verriet, "A Holonic Approach to Warehouse Control," *Proc. Int. Conf. on Practical Appl. of Agents and Multiagent Systems*, pp. 1-10, Spain, 2009.

[5] H. van Brussel, J. Wyns, P. Valckenaers, L. Bongaerts, P. Peeters, "Reference Architecture for Holonic Manufacturing Systems: PROSA," *Computers in Industry*, Vol. 37, No. 3, pp. 255–276, 1998.

[6] A. Giret, V. Botti, "Holons and agents," *Journal of Intelligent Manufacturing*, Vol. 15, No. 5, pp. 645–659, 2004.

[7] Z. Wang, Y. Takano, Y. Hirata, K. Kosuge, "Decentralized Cooperative Object Transportation by Multiple Mobile Robots With a Pushing Leader," in *Distributed Autonomous Robotic Systems 6*, Springer Japan, pp. 453–462, 2007.

[8] R.W. Brockett, "Asymptotic stability and feedback stabilization," in R.W. Brockett, R.S. Milman, H.J. Sussmann (Eds.), *Differential Geometric Control Theory*, Birkhauser, Boston, 1983, pp. 181–191.

[9] Y. Kanayama, Y. Kimura, F. Miyazaki, T. Noguchi, "A Stable Tracking Control Method for an Autonomous Mobile Robot," *Proc. IEEE Int. Conf. Rob. Automat.*, pp. 384–389, Cincinnati, OH, 1990.

[10] Z.-P. Jiang, E. Lefeber, H. Nijmeijer, "Saturated Stabilization and Tracking of a Nonholonomic Mobile Robot," *Systems & Control Letters*, Vol. 42, pp. 327–332, 2001.

[11] D. Kostić, S. Adinandra, J. Caarls, N. van de Wouw, H. Nijmeijer, "Collision-free Tracking Control of Unicycle Mobile Robots," *accepted for IEEE Int. Conf. Dec. Control*, Shanghai, China, 2009.

[12] J.C. Latombe, *Robot Motion Planning*, Kluwer Academic Publishers, Boston, MA, 1991.

[13] V.M. Popov, *Hyperstability of Control Systems*, Springer-Verlag, Berlin, 1973.

[14] F. Mondada, M. Bonani. *E-puck education robot*, 2007. http://www.e-puck.org

Preprint submitted to 2010 American Control Conference.
Received September 28, 2009.